Large-scale arrays of picolitre chambers for single-cell analysis of large cell populations†

Won Chul Lee,[ab] Sara Rigante,[b] Albert P. Pisano*[b] and Frans A. Kuypers*[a]

Received 22nd June 2010, Accepted 6th August 2010
DOI: 10.1039/c0lc00139b

We present a new method to analyze the cytoplasmic contents of single cells in large cell populations. This new method consists of an array of microchambers in which individual cells are collected, enclosed, and lysed to create a reaction mixture of the cytoplasm with extracellular detection agents. This approach was tested for the analysis of red blood cells in 10 000 microchambers in parallel. Single cells were routinely collected in more than 60% of microchambers, the collected cells were robustly (up to 99%) lysed by electric fields, and the cytoplasm enclosed in each microchamber was analyzed with fluorescence microscopy. Using a heterogeneous cell mixture, we verified that the new method could distinguish individual cells by cytoplasmic composition and the analysis compared well with conventional flow-cytometric evaluation of mixed cell populations. In contrast to flow-cytometry, the new method monitored single cells over time, thus characterizing the distributions of caspase activities of 5000 individual cells. This approach should be interesting for a variety of applications that would benefit from the ability to measure the distribution of cytoplasmic compounds in complex cell populations, including hematology, oncology, and immunology.

Introduction

Single-cell analysis has become an important tool for characterizing cellular contents in cell populations.[1,2] Unlike bulk experiments that rely on averaging entire populations, single-cell approaches analyze large numbers of individual cells and determine the distributions of cellular properties. Such distributions in cell populations turn out to be a hallmark of physiology and pathology,[3,4] and have been defined with current techniques including flow-cytometry,[5–7] laser scanning cytometry,[8–10] and automated microscopy.[7,11–14] However, these techniques are mainly used to define cell surface markers,[3,6] as only limited probes are available that penetrate the cell membrane for measurement of cytoplasmic compounds. For the detection of other cytoplasmic compounds, cells need to be permeabilized[11] or modified[5,7,13,14] to express fluorescence, which changes the cell physiology.[3] Methods based on single-cell lysis[15–21] have been used to avoid these issues, but are impractical as a method to measure a significant number of cells in a reasonable amount of time for establishing statistically relevant distributions within a large cell population. The measurement of enzyme activity in single cells adds further complexity, as it requires monitoring of substrate use over time under well-defined conditions.

To address these limitations, we present a novel approach using large-scale arrays of microchambers to allow cytoplasmic characterization of individual cells. As proof of principle, we use arrays with approximately 10 000 microchambers (approximately 1000 fl each) in which individual red blood cells (90 fl) are lysed, leading to a defined dilution of the cytoplasm in a reaction mixture of choice. The concept is depicted in Fig. 1. Cells are collected into open microwells, which are covered to form closed microchambers. The isolated cells are electrically lysed, followed by measurement of a chemical reaction in the microchambers.

Compared to previously reported single-cell arrays[4,9,10,12,22–27] and liquid–liquid droplet microfluidics,[28–31] this method enables lysis of individual cells in closed volumes. In contrast to other microfluidic approaches,[11,15–21,32] this method offers the rapid collection of cells from an out-of-plane (vertical) direction

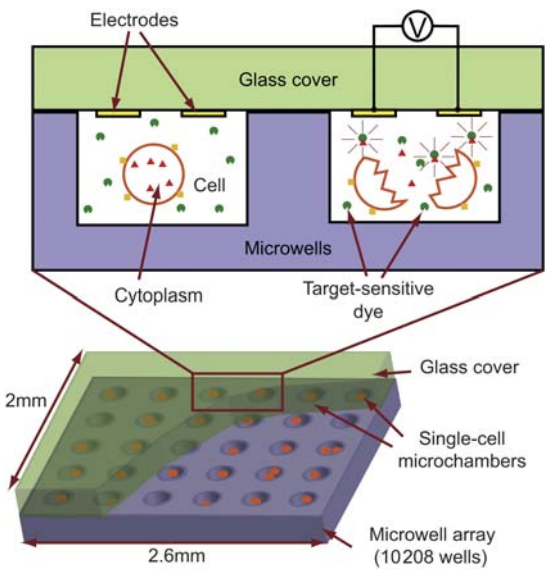

Fig. 1 Single-Cell Microchamber Array (SiCMA). In each microchamber, an individual cell is collected, enclosed, and lysed to create a reaction mixture of the cytoplasm with extracellular detection agents.

[a]*Children's Hospital Oakland Research Institute, 5700 Martin Luther King Jr Way, Oakland, California, 94609, USA. E-mail: fkuypers@chori.org; Fax: +1-510-450-7910; Tel: +1-510-450-7620*
[b]*Berkeley Sensor & Actuator Center, University of California at Berkeley, Berkeley, California, 94720, USA. E-mail: appisano@me.berkeley.edu; Fax: +1-510-642-6163; Tel: +1-510-643-7013*
† Electronic supplementary information (ESI) available: Six figures and a video of detailed experimental results. See DOI: 10.1039/c0lc00139b

without complex microfluidic channels and valves. The simplicity of fully closed chambers sacrifices the ability of adding and manipulating chemical reagents after closure, but offers rapid measurements of a much larger cell number. By simply choosing the array size, populations of 100 000 cells measured in parallel are easily attainable. Analysis of such large numbers of cells can be used to define the distribution of entities in cell populations similar to flow-cytometry. As in flow-cytometry surface markers can be defined, but in contrast to flow-cytometry a larger set of cellular probes can be used to measure cytoplasmic compounds. Moreover, individual cells can be measured over time, allowing enzymology of single cells in large populations.

Results and discussion

To test the concept, we designed and fabricated a single-cell microchamber array (SiCMA) composed of a microwell array (88 by 116, total 10 208 wells) and a glass cover with gold electrodes (Fig. 1 and S1†). The five-step working principle is illustrated (see *Experimental* and Fig. 2) using red blood cells (RBCs). In the first step, cells were loaded by dropping a RBC suspension on the top of the microwell array.[9,12,22,23] A simple flow of buffer across the top removed cells not trapped in the microwells. As shown in the optimization results (Fig. 3A), most microwells (83.3 ± 3.0%) contained a single cell, while the remaining wells were empty or showed the presence of more than one cell (see *Experimental* and Fig. 3B). In the second step, a glass plate with electrodes was placed on top of the wells to create closed microchambers, where liquid solutions could be enclosed without leaks for an hour.[33] The pitch of wells and electrodes was chosen such that alignment was not needed. While the closing of the chambers removed some cells from the wells, more than 60% of 10 208 chambers routinely contained single cells (see *Experimental* and Fig. 3C). In the third step, automated image analysis defined the

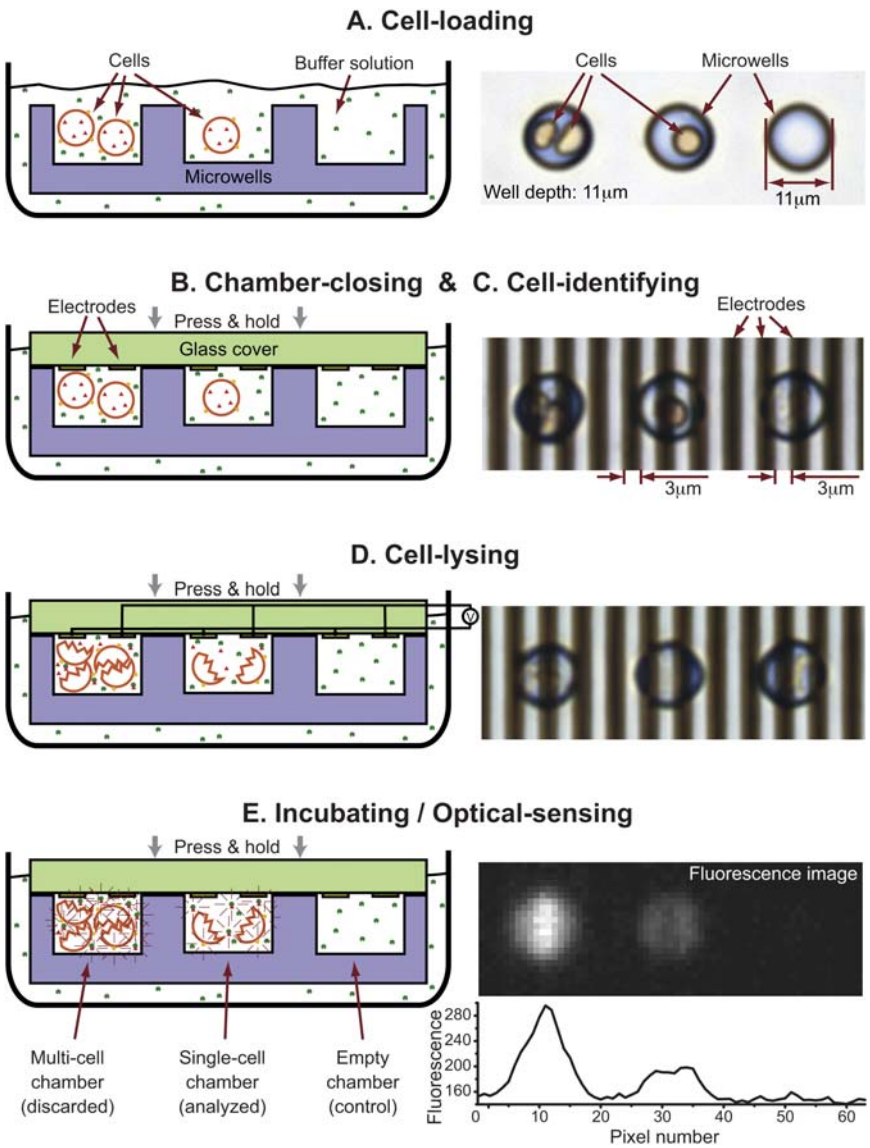

Fig. 2 The five-step operations illustrated by cartoon images (left) and microscopic images (right). (A) Cells are seeded on a microwell array. (B) Microwells are covered to form closed microchambers. (C) Cells in each microwell are identified. (D) An electrical pulse is applied to lyse the cell and mix its contents with the surrounding medium. (E) The ensuing chemical reaction is monitored by fluorescence.

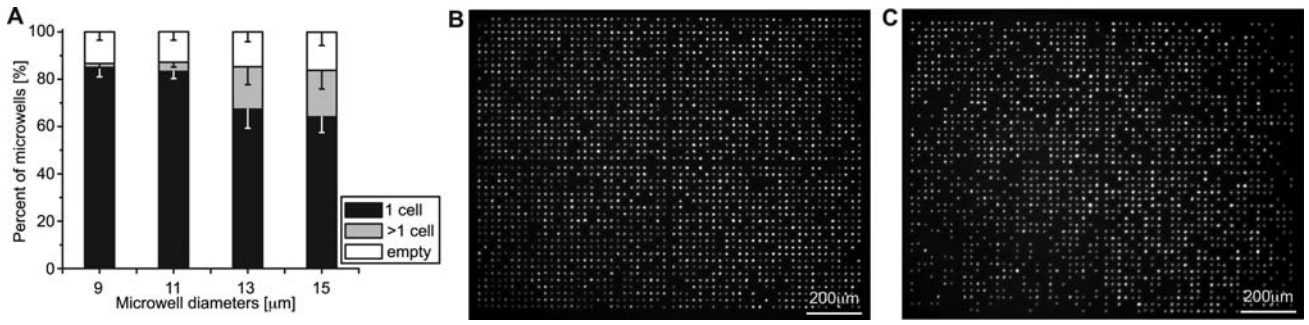

Fig. 3 Single-cell collection in the microchamber array. (A) Cell occupancy as a function of microwell diameters after the cell loading. (B) Loaded cells on the microwell array. 86.0% of 2552 wells (1/4 of a total area) contained single cells. (C) Captured cells in the microchamber array after the chamber-closing. 67.1% of 2552 chambers (1/4 of a total area) contained single cells. Repeated measurements (10 times) showed the single-cell occupancy of 65.4 ± 7.8% after the chamber-closing. (B) and (C) were visualized by the fluorescence microscopy of APC tagged cells.

presence of cells in each chamber (Fig. S2†). Thus, microchambers with single cells can be differentiated from those with no or multiple cells. Subsequently in the fourth step, a voltage pulse was applied across the electrodes to disrupt the plasma membrane and the cytoplasm mixed with the surrounding medium (Movie S1†). In the fifth and final step, the optical signal resulting from the mixture of cytoplasm and detection agents was recorded separately for each chamber (Fig. S3†). The optical signal represented the amount of target cytoplasmic compounds in single cells. The concentration of the cytoplasmic compounds can be obtained with additional fluorescence dyes that can monitor the volume of single cells.

To verify the ability to measure cellular characteristics in a heterogeneous population, we used a heterogeneous mixture of RBC. One portion of RBC was labeled with the fluorescently red labelled allophycocyanin (APC), and a second portion was loaded with the fluorescently green calcium indicator Fluo-4. The mixture of APC and Fluo-4 cells was suspended in a calcium-containing buffer. Since the fluorescence of Fluo-4 is strongly dependent on the calcium concentration, the low calcium concentration inside normal RBC results in low green fluorescence of intact Fluo-4 cells. The lysis of Fluo-4 cells generates strong green fluorescence due to the extracellular calcium. The mixed cells were sub-optimally loaded in the array on purpose,

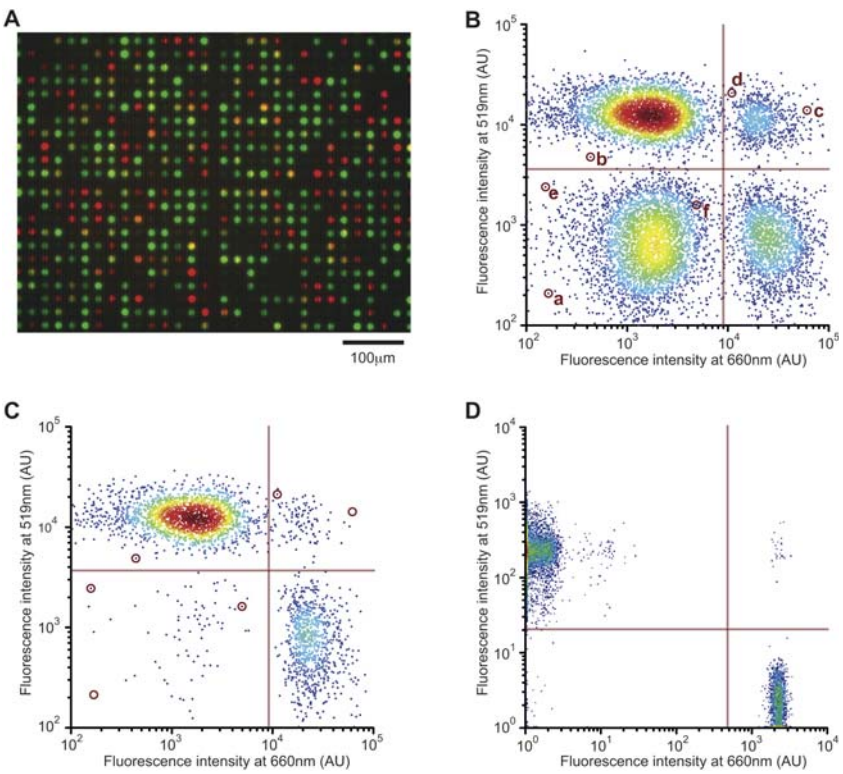

Fig. 4 Multicolor single-cell analysis of a mixed cell population. (A) Image of 1/16 of the SiCMA device (628 microchambers) showing red or green fluorescence after lysis of the cells. (B) Dot plot of the fluorescence intensity in each of 10 208 microchambers. (C) Dot plot of the fluorescence intensity after removal of microchambers with one or multiple cells from the data in (B). (D) Two-color flow-cytometric analysis of the same cell population.

resulting in a significant number of chambers with either zero or multiple cells. After closing of the microchambers, image analysis in normal light determines the presence of cells in the chambers. Sub-optimal loading allowed us to test the performance of the image analysis software in its ability to distinguish the presence and number of cells in each chamber. Fluorescence analysis determined chambers that contained APC labeled cells (red) or damaged Fluo-4 cells (green) before electrical disruption of the membrane. Less than 0.1% of the chambers showed high green fluorescence, indicating low cell damage during the loading and closure procedures (Fig. S3†). Fluorescence analysis after electrical disruption of the membrane showed that chambers with APC cells were still red, chambers with Fluo-4 cells turned green, and chambers with both APC and Fluo-4 cells appeared yellow (Fig. 4A). Histograms (Fig. S4†) and two-dimensional dot plots (Fig. 4B) were generated based on fluorescence intensity of each chamber (event). Fig. 4B shows a typical experiment with upper-left (UL, green), upper-right (UR, yellow), lower-left (LL, dark), and lower-right (LR, red) quadrants that contained 3702 (UL), 761 (UR), 3806 (LL), and 1939 (LR) events, respectively.

The image analysis software (see *Experimental*) was programmed to identify "no cell", "single cell", and "multiple cell" events based on microchamber images captured before the cell lysis. Applying the image analysis effectively removed events in the LL (no cell) and UR (both Fluo-4 and APC cells) quadrants (Fig. 4C and S5†). Of the 4567 events in the LL and UR quadrants, only 187 or 4% were not removed by image recognition, and manual analysis of these events showed that the majority were empty chambers or chambers with multiple cells recognized incorrectly due to unwanted shadows of electrodes or other defects (events d and e, Fig. S2D and S2E†). Similarly, multi-cell events were effectively removed from the UL and LR quadrants leaving 2133 and 864 events, respectively. Only in 19 events (0.6%), cells were not lysed (event f, Fig. S2F†) under the electrical conditions chosen.

These results show that, even with sub-optimal loading, statistically relevant data can be collected on cell populations using image analysis. Flow-cytometric analysis of the same population was also performed after incubation with the calcium ionophore A23187 (Sigma), generating strong green fluorescence in the Fluo-4 loaded cells. The flow-cytometric data (Fig. 4D) indicated a 1 to 2.46 ratio of APC to Fluo-4 cells in this mixture, which correlated well with the SiCMA data (1 : 2.47 ratio). Together, these experiments indicate that this new method is able to distinguish individual cells in mixed populations, is able to detect cytoplasmic compounds, and that the analysis compares well with well-established flow-cytometric evaluation of mixed cell populations.

In contrast to flow-cytometry, this approach can readily monitor single cells over time, allowing the measurement of enzyme activities by definition of substrate breakdown or product formation. To illustrate this, we measured caspase 3 activity with a fluorogenic substrate (Z-DEVD-R110, Molecular Probes). Caspase activity leads to the breakdown of this substrate and an increase in fluorescence at 520 nm. RBCs in which caspase 3 was activated were loaded into microchambers in a buffer containing Z-DEVD-R110. Fluorescence intensities were compared between microchambers with no and single cells after electrical disruption of the RBC membranes (Fig. 5A). Immediately after the cell lysis, both empty chambers and chambers with a single cell exhibited low fluorescence (235 ± 193 and 308 ± 304 AU, respectively), indicating low substrate breakdown. While empty microchambers maintained low fluorescence, microchambers with lysed single cells generated an increase in fluorescence over time, as the breakdown of the substrate by caspase released from the cytoplasm progressed (Fig. 5A and S6†). Analysis of fluorescence increase in each microchamber allowed us to define enzyme activity of single cells in cell populations (examples shown in Fig. 5B). Under the conditions chosen, fluorescence increase was linear in virtually all microchambers over the 30 minutes of measurement. A histogram of the fluorescence increase rates during the 30 min incubation (Fig. 5C) represents the distribution of the relative caspase activity in single cells in the total cell population (5102 cells).

In conclusion, we present a novel approach to analyze the cytoplasm of single cells in heterogeneous cell populations. We envision that the single-cell microchamber array or SiCMA can be used in a variety of applications that would benefit from the ability to measure the distribution of cytoplasmic compounds or enzyme activities in complex cell populations, including hematology, oncology, and immunology.

Experimental

Device fabrication

PDMS (polydimethylsiloxane) microwell arrays and glass covers with electrodes were fabricated using conventional micromolding and micromachining techniques. Masters for the

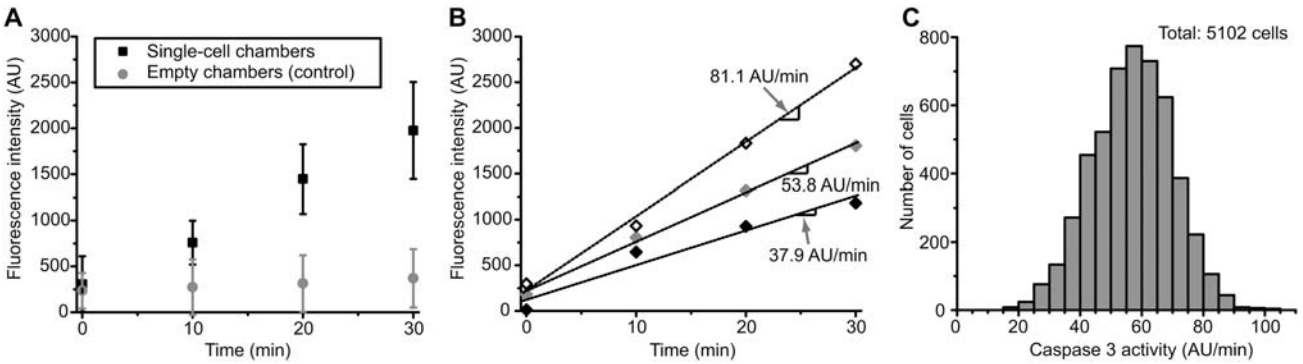

Fig. 5 Caspase 3 activity of single cells. (A) Fluorescence signals in time in empty microchambers (●) and microchambers with single cells (■). (B) Three examples of fluorescence signals in individual microchambers with single cells. Caspase activity expressed as an increase rate of fluorescence in time is indicated. (C) Distribution of caspase 3 activity in all microchambers with single cells.

microwell arrays were made from photolithographic patterns of SU8-2010 (MicroChem) on silicon wafers. PDMS was poured over the master and then degassed before curing. After curing, the PDMS microwell arrays were peeled off. Glass covers with Cr/Au electrodes were fabricated with a lift-off process. Photoresists, LOR-10A (MicroChem) and S1818 (Rohm and Haas), were patterned on a glass wafer, and then Cr/Au layers (10nm/120nm) were thermally evaporated on the wafer. Finally, photoresist removal defined Cr/Au patterns for electrodes on the glass wafer. The PDMS microwell arrays were treated with a high frequency generator (BD-10AS, Electro-Technic Products) to avoid trapping of air bubbles in microwells. The microwell arrays were blocked with 0.5 mg mL^{-1} bovine serum albumin and rinsed with Hepes-buffered saline (HBS) before use.

Sample preparation

Whole blood from healthy volunteers was drawn in acid citrate dextrose (ACD) after obtaining informed consent using an IRB approved protocol. Red blood cells were separated by centrifugation and washed with Hepes-buffered saline (HBS, 10 mM Hepes, pH 7.4, and 145 mM NaCl) by repeated centrifugation and aspiration of the supernatant. The red blood cells were re-suspended at 5% hematocrit in buffer HBSF (10 mM Hepes, pH 7.4, 145 mM NaCl, 0.15 mM $MgCl_2$, 5 mM glucose, and 5 mM inosine) and stored at 4 °C until use within 48 h. Before use, cells were suspended in buffer at room temperature to a cell concentration as indicated.

Cell loading

A drop of a red blood cell suspension (0.2% hematocrit) was applied to the top of a microwell array, resulting in the entrapment of cells in microwells as previously reported.[9,12,22,23] After allowing the cells to settle for 15 min, a simple flow of buffer across the top removed cells not trapped in the microwells. In order to maximize the single-cell occupancy in microwells, we tested microwells that had various diameters (9, 11, 13, and 15 μm) and a fixed depth (11 μm). For each kind of microwell arrays, 10 prototypes of 100 microwells were observed with optical microscopy after the cell loading. As indicated in Fig. 3A, microwells with diameters of 9 μm and 11 μm showed high single-cell occupancies of 85.0 ± 4.0% and 83.3 ± 3.0%, respectively. These results coincided well with that of the previous research achieved with the single-cell occupancies of 80–90% in 20 000–30 000 microwells.[9,12,22,23] For the simple fabrication, we chose a larger diameter and performed further analysis with microwells whose diameter was 11 μm. Fig. 3B shows an example of the cell-loading results on a large-scale (2552 wells) array of microwells.

Chamber closing

The PDMS microwell array was placed in a Petri dish before the cell loading as shown in Fig. 2. After the cell loading, a buffer solution with detection agents was added to the Petri dish so that the microwell was immerged in the buffer. A glass cover with the electrode pattern was attached to a microstage and placed on top of the microwell. For the attachment, we used a thick (1 cm) PDMS block between the cover and the stage. This soft block enabled perfect enclosure of all chambers even if the microwell array and the cover were not parallel. Then, we moved down the glass cover gently with the microstage to close the microwells. The cover was pressed and hold with a pressure of 10 ± 5 kPa to avoid leakage from the chambers. After this chamber-closing step, the microchambers were ready to be analyzed.

As indicated in *Results and discussion*, the closing of the chambers removed some cells from the microwells that contained cells. This effect was quantified with microscopic observations before and after the chamber closing. From 10 repeated measurements with 100 microwells, we verified that 21.3 ± 10.0% of cells were removed from the microwells, and finally 65.4 ± 7.8% of the closed microchambers contained single cells. This level (~60%) of the single-cell occupancy was also achieved in large-scale arrays, as shown in Fig. 3C. Thus, by simply increasing the array size to 20 000 microwells, populations of 10 000 single cells are easily attainable. Such numbers allow the measurement of distribution curves in large cell populations.

Image acquisition

The device was mounted on an inverted fluorescence microscope (Olympus IX 70) equipped with a Photometrics Coolsnap FX camera (1 M pixel CCD). Sixteen bright-field images of 628 microchambers were captured to cover entire 10 208 microchambers for cell identification. Each microchamber was shown in a 20 by 20 pixel image, with the minimum resolution for the current cell-identification software. For opto-chemical analysis, four fluorescence images of 2552 microchambers were captured. Each of the four quadrants of the device has its own electrodes, which made it possible to individually lyse the cells in each quadrant and follow fluorescence changes in time after the electrical cell lysis.

Cell identification with image analysis

We developed a simple program to identify cells in microchambers (Fig. 2) with MATLAB (The Mathworks).[34] This program used the bright-field images of the microchamber arrays that were captured before the cell lysis. First, periodic patterns of electrodes and microchambers were recognized and excluded in the analysis. Subsequently, cell areas (pixels) were defined based on dark or yellow colors using the image segmentation by optimum global thresholding.[34] From these pixels, cell areas and area moments of inertia (MOI) were calculated. The cell areas defined the presence of cells or empty chambers, and the MOIs differentiated microchambers with single cells from those with multiple cells. In some cases, shadows from electrodes interfered in the recognition process in the low-resolution images. In order to evaluate the program, we manually counted cells in the microchambers and compared the result with that of the image analysis program. The 8 repeated comparisons of 29 microchambers showed that 16.4 ± 8.4% of events were misidentified. In addition, most of these misidentified events were excluded in the final result. Only 3.0 ± 3.9% of events remained and generated errors since they were no-cell or multi-cell events that were misidentified as single-cell events.

Cell lysis

A 0.2 second pulse of a 36.8 Vpp, 2 MHz AC signal was applied to the 3 μm gap electrodes. Cells were attracted to the electrodes

by positive DEP (dielectrophoretic) force[35–37] within the first 0.1 s and lysed at the position of the maximum electric field. The two buffers in our test have conductivities of 1.535 mS cm^{-1} (10 mM Hepes, pH 7.4, 190 mM sucrose, 0.5 mg mL^{-1} BSA, 8 mM NaCl, and 1 mM $CaCl_2$) and 1.521 mS cm^{-1} (10 mM Hepes, pH 7.4, 190 mM sucrose, 0.5 mg mL^{-1} BSA, 9 mM NaCl, 5 mM DTT (dithiothreitol), and 25 μM Z-DEVE-R110 (Molecular Probes/Invitrogen)), respectively, optimal for lysis of red blood cells in this electrical field.[20,21,35,37–40]

APC labeling[41]

Allophycocyanin (APC) tagged cells were prepared by labeling with APC streptavidin of red blood cells biotinylated by incubation for 15 min at 37 °C with 0.9 mM EZ-link Sulfo-NHS-LC-biotin (Pierce) at 5% hematocrit in HBSF. After three washes in HBSF, the biotinylated cells were incubated with APC-conjugated streptavidin (Molecular Probes/Invitrogen) at 0.25 μg mL^{-1}. The APC tagged RBCs were washed and resuspended at 0.2% hematocrit in working buffers.

Fluo-4 loading[41]

Red cells were resuspended at 0.4% hematocrit in buffer B (10 mM Hepes, pH 7.4, 70 mM NaCl, 80 mM KCl, 0.15 mM $MgCl_2$, 0.1 mM EGTA, 10 mM inosine, and 5 mM pyruvic acid) to preserve ATP levels during the Fluo-4 loading procedure. Fluo-4 AM (Molecular Probes/Invitrogen) was added at a final concentration of 2.5 μM and the cells were incubated for 1 h at 37 °C, followed by two wash steps in HBSF.

Calcium loading[41]

Red blood cells were incubated for 10 min at 37 °C with 400 nM calcium ionophore A23187 (Sigma) in 1 mM calcium. The suspensions were then placed at room temperature in the dark and evaluated within 20 min by flow-cytometry.

Flow-cytometry

Flow-cytometric analysis was performed on a FACS Calibur flow cytometer (Becton Dickinson). Flowjo software (FlowJo) was used for data analysis.

Caspase 3 activation in RBC[42]

Caspase 3 in red blood cells was activated by *t*-BHP (*tert*-butylhydroperoxide) treatment. Red blood cells (5% hematocrit) were treated with 3 mM *t*-BHP for 60 min. The cells were washed three times in a five-fold volume of HBS, resuspended in the working buffer, and kept on ice for further analysis.

Acknowledgements

This work was supported by the US National Institutes of Health R21 (5R21HL092535-02) and SBIR (1R43GM090515-01) programs. We thank E. Soupene, S. Larkin, and T. Brackbill for performing flow-cytometric study and providing useful discussions.

References

1 K. Cottingham, *Anal. Chem.*, 2004, **76**, 235A–238A.
2 N. d. Souza, *Nat. Methods*, 2010, **7**, 35–35.
3 B. F. Brehm-Stecher and E. A. Johnson, *Microbiol. Mol. Biol. Rev.*, 2004, **68**, 538–559.
4 D. Di Carlo and L. P. Lee, *Anal. Chem.*, 2006, **78**, 7918–7925.
5 J. R. S. Newman, S. Ghaemmaghami, J. Ihmels, D. K. Breslow, M. Noble, J. L. DeRisi and J. S. Weissman, *Nature*, 2006, **441**, 840–846.
6 H. M. Shapiro, *Practical Flow Cytometry*, Wiley-Liss, New York, 4th edn, 2003.
7 J.-Q. Wu and T. D. Pollard, *Science*, 2005, **310**, 310–314.
8 M. M. Harnett, *Nat. Rev. Immunol.*, 2007, **7**, 897–904.
9 Y. Tokimitsu, H. Kishi, S. Kondo, R. Honda, K. Tajiri, K. Motoki, T. Ozawa, S. Kadowaki, T. Obata, S. Fujiki, C. Tateno, H. Takaishi, K. Chayama, K. Yoshizato, E. Tamiya, T. Sugiyama and A. Muraguchi, *Cytometry, Part A*, 2007, **71**, 1003–1010.
10 A. Jin, T. Ozawa, K. Tajiri, T. Obata, S. Kondo, K. Kinoshita, S. Kadowaki, K. Takahashi, T. Sugiyama, H. Kishi and A. Muraguchi, *Nat. Med.*, 2009, **15**, 1088–1092.
11 L. Cai, N. Friedman and X. S. Xie, *Nature*, 2006, **440**, 358–362.
12 X. A. Figueroa, G. A. Cooksey, S. V. Votaw, L. F. Horowitz and A. Folch, *Lab Chip*, 2010, **10**, 1120–1127.
13 A. Gordon, A. Colman-Lerner, T. E. Chin, K. R. Benjamin, R. C. Yu and R. Brent, *Nat. Methods*, 2007, **4**, 175–181.
14 J. M. Levsky, S. M. Shenoy, R. C. Pezo and R. H. Singer, *Science*, 2002, **297**, 836–840.
15 J. W. Hong, V. Studer, G. Hang, W. F. Anderson and S. R. Quake, *Nat. Biotechnol.*, 2004, **22**, 435–439.
16 B. Huang, H. Wu, D. Bhaya, A. Grossman, S. Granier, B. K. Kobilka and R. N. Zare, *Science*, 2007, **315**, 81–84.
17 E. A. Ottesen, J. W. Hong, S. R. Quake and J. R. Leadbetter, *Science*, 2006, **314**, 1464–1467.
18 N. M. Toriello, E. S. Douglas, N. Thaitrong, S. C. Hsiao, M. B. Francis, C. R. Bertozzi and R. A. Mathies, *Proc. Natl. Acad. Sci. U. S. A.*, 2008, **105**, 20173–20178.
19 J. F. Zhong, Y. Chen, J. S. Marcus, A. Scherer, S. R. Quake, C. R. Taylor and L. P. Weiner, *Lab Chip*, 2008, **8**, 68–74.
20 M. A. McClain, C. T. Culbertson, S. C. Jacobson, N. L. Allbritton, C. E. Sims and J. M. Ramsey, *Anal. Chem.*, 2003, **75**, 5646–5655.
21 H.-Y. Wang and C. Lu, *Chem. Commun.*, 2006, **33**, 3528–3530.
22 J. R. Rettig and A. Folch, *Anal. Chem.*, 2005, **77**, 5628–5634.
23 S. Yamamura, H. Kishi, Y. Tokimitsu, S. Kondo, R. Honda, S. R. Rao, M. Omori, E. Tamiya and A. Muraguchi, *Anal. Chem.*, 2005, **77**, 8050–8056.
24 J. C. Love, J. L. Ronan, G. M. Grotenbreg, A. G. van der Veen and H. L. Ploegh, *Nat. Biotechnol.*, 2006, **24**, 703–707.
25 A. O. Ogunniyi, C. M. Story, E. Papa, E. Guillen and J. C. Love, *Nat. Protocols*, 2009, **4**, 767–782.
26 C. M. Story, E. Papa, C.-C. A. Hu, J. L. Ronan, K. Herlihy, H. L. Ploegh and J. C. Love, *Proc. Natl. Acad. Sci. U. S. A.*, 2008, **105**, 17902–17907.
27 Q. Han, E. M. Bradshaw, B. Nilsson, D. A. Hafler and J. C. Love, *Lab Chip*, 2010, **10**, 1391–1400.
28 E. Brouzes, M. Medkova, N. Savenelli, D. Marran, M. Twardowski, J. B. Hutchison, J. M. Rothberg, D. R. Link, N. Perrimon and M. L. Samuels, *Proc. Natl. Acad. Sci. U. S. A.*, 2009, **106**, 14195–14200.
29 M. Chabert and J.-L. Viovy, *Proc. Natl. Acad. Sci. U. S. A.*, 2008, **105**, 3191–3196.
30 A. Huebner, M. Srisa-Art, D. Holt, C. Abell, F. Hollfelder, A. J. deMello and J. B. Edel, *Chem. Commun.*, 2007, **12**, 1218–1220.
31 P. Kumaresan, C. J. Yang, S. A. Cronier, R. G. Blazej and R. A. Mathies, *Anal. Chem.*, 2008, **80**, 3522–3529.
32 G. J. Shah, A. T. Ohta, E. P.-Y. Chiou, M. C. Wu and C.-J. C. J. Kim, *Lab Chip*, 2009, **9**, 1732–1739.
33 Y. Rondelez, G. Tresset, K. V. Tabata, H. Arata, H. Fujita, S. Takeuchi and H. Noji, *Nat. Biotechnol.*, 2005, **23**, 361–365.
34 R. C. Gonzalez, R. E. Woods and S. L. Eddins, *Digital Image Processing using MATLAB*, Pearson Prentice Hall, Upper Saddle River, NJ, 2004.
35 P. T. Lynch and M. R. Davey, *Electrical Manipulation of Cells*, Chapman & Hall, New York, 1996.
36 X. B. Wang, Y. Huang, X. Wang, F. F. Becker and P. R. Gascoyne, *Biophys. J.*, 1997, **72**, 1887–1899.
37 U. Zimmermann and G. A. Neil, *Electromanipulation of Cells*, CRC Press, Boca Raton, FL, 1996.

38 F. Han, Y. Wang, C. E. Sims, M. Bachman, R. Chang, G. P. Li and N. L. Allbritton, *Anal. Chem.*, 2003, **75**, 3688–3696.
39 Y. Nashimoto, Y. Takahashi, T. Yamakawa, Y.-S. Torisawa, T. Yasukawa, T. Ito-Sasaki, M. Yokoo, H. Abe, H. Shiku, H. Kambara and T. Matsue, *Anal. Chem.*, 2007, **79**, 6823–6830.
40 L. D. Oliver and H. G. L. Coster, *Bioelectrochemistry*, 2003, **61**, 9–19.
41 K. de Jong and F. A. Kuypers, *Cytometry, Part A*, 2007, **71**, 693–699.
42 D. Mandal, P. K. Moitra, S. Saha and J. Basu, *FEBS Lett.*, 2002, **513**, 184–188.

